Journal Homepage: http://ijcpe.uobaghdad.edu.iq
Iraqi Journal of Chemical and Petroleum Engineering
Vol. 27 No. 2 (June 2026) 123 – 137
EISSN: 2618-0707, PISSN: 1997-4884

Synthesis of nanoporous SnO_2 anode by anodization in a rotating cylinder configuration

Ghaidaa A. Ismael [a, *] , **Ali H. Abbar** [a]

a Department of Biochemical Engineering, Al-Khwarizmi college of Engineering, University of Baghdad, Baghdad, 10071, Iraq

Abstract

Nanoporous-SnO_2 films were electrochemically prepared via anodizing of metallic tin electrodeposited on a cylindrical copper substrate using rotating cylinder electrode Technique. The effects of anodizing potential (4-7V), oxalic acid (OA) concentration (0.1-0.5M), time (10-20), and rotation speed (150-450 rpm) on the electrochemical activity of SnO_2 as an anode in degrading methylene blue (MB) were investigated. Results showed that increasing oxalic acid concentration gives better performance in degrading MB while increasing anodizing potential enhanced the electrode activity up to a potential of 5 V beyond which no enhancement of electrode activity towared MB degradation was noted. Longer time of anodizing has opposite effect while rotation speed enhanced the electrocatalytic activity of SnO_2. The best conditions of anodizing were potential of 5 V, 0.4M OA, 15 min, and 250 rpm in which MB removal was 87.6%. Structural morphology of SnO_2 prepared at the optimum conditions confirmed the conversion of tin to SnO_2 with free crack structure. These results demonstrate that adopting anodizing method with rotating cylinder technique to forming SnO_2 anodes is a promising strategy for constructing high-performance anodes suitable for treatment wastewaters.

Keywords: Nanoporous film; Tin oxide; Anodization; Oxalic acid; Methylene blue; Rotating cylinder electrode.

Received on 25/04/2026, Received in Revised Form on 07/06/2026, Accepted on 07/06/2026, Published on 30/06/2026

https://doi.org/10.31699/IJCPE.2026.2.10

1- Introduction

Tin dioxide (SnO_2) is a semiconductor with a wide energy gap (≈3.6 eV) and unique electronic, optical, and catalytic properties [1], making it a promising material for various applications, including gas sensor applications [2], solar cells [3], and lithium ion batteries [4]. The efficiency of these applications depends directly on the "morphology" and size of the surface area. Nanoporous structures provide faster pathways for charge transport and more efficient surface interactions thus enhancing the functional performance of these materials [5]. SnO_2 anodes can be prepared by various methods including thermal decomposition, hydrothermal synthesis, sol-gel, and anodizing [6-8].

Electrochemical anodizing has emerged as a simple and efficient method for producing porous oxide nanolayers [9]. Feng et al. [10] have shown that anodization of tin in selected electrolytes results in the creation of flowered patterns or nanoribbons, multiplying several times the surface area. Leszek et al. [11] also investigated growth mode during anodizing and demonstrated a delicate balance between oxide layer formation and chemical dissolution of the oxides by an acid is required to form pores and showed that anodizing conditions (applied voltage, electrolyte concentration, and processing time) in oxalic solutions directly affect pore diameter and regularity, with increasing voltage leading to larger channels and thinner walls, but with the potential for cracking. This aligns with Cao et al. [12] findings about the electrolyte type (e.g., fluoride and sulfide) regulation of pore diameter and regularity.

The Anodizing technique has demonstrated that it is capable of producing highly ordered SnO_2 films. For example, Yamaguchi et al. [13] demonstrated the fabrication of a transparent SnO_2 nanoelectrode with 50 nm columnar pore structures and presented its high electrochemical activity. Likewise (to exhibit the benefit of adhesion), Shin et al. [14] reported a new technique for the preparation of Ag-doped SnO_2 nanowires on copper substrates as flexible, binder-free electrodes for Lithium batteries, while experimentally demonstrating that direct anodization could provide better mechanical strength and charge-transfer ratios compared to sintered powder bonds.

Notwithstanding these advancements, existing research has concentrated on the anodization of tin foils, with the synthesis of SnO_2 on conductive substrates such as copper remaining limited investigated [10, 13]. Although copper exhibits superior electrical conductivity and high mechanical properties, the development of stable oxide films on its surface requires interfacial engineering strategies to mitigate delamination and achieve uniformity. Significantly, the role of hydrodynamic parameters during anodization particularly the implementation of rotating cylindrical electrode (RCE) effect on pore morphology and film homogeneity has not

*Corresponding Author: Email: Ghaidaa.Anas2405m@kecbu.uobaghdad.edu.iq

been sufficiently characterized in the current literature. Consequently, this research aims to address this gap through the implementation of a defined two-step fabrication strategy comprising tin electrodeposition followed by electrochemical anodization for the preparation of nanoporous SnO_2 films on copper substrates utilizing an RCE system.

RCE anodes were used successfully in treating various types of wastewaters because of attaining high mass transfer generated by turbulence flow under moderate speed of rotation for these anodes with the easiness of their application on the industrial scales [15-17]. Furthermore, Rotational dynamics are enhancing ionic mass transfer, minimize localized gas bubble accumulation, and promote the development of uniform nanostructures [18]. The present study systematically examines the influence of applied potential, electrolyte concentration, rotational velocity, and time on the film morphology and structural integrity. Additionally, the electrochemical activity of the synthesized electrodes is evaluated via methylene blue dye degradation, thus establishing a reliable approach for advanced environmental remediation applications.

2- Experimental work

2.1. Chemicals

Chemical used in this research were tin chloride dihydrate ($SnCl_2 \cdot 2H_2O$, Thomas Baker, India), hydrochloric acid (HCl, 35–38%, Thomas Baker, India), trisodium citrate dihydrate ($C_6H_5Na_3O_7 \cdot 2H_2O$, ACS Chemicals, India), thiourea (NH_2CSNH_2, Thomas Baker, India), oxalic acid dihydrate ($COOH_2 \cdot 2H_2O$, Hopkin & Williams, England),methylene blue (MB) with 97% purity (BDH chemical Ltd pool England) and sodium sulfate (Na_2SO_4) added as a supporting electrolyte to improve ionic conductivity. All aqueous solutions were prepared using deionized water.

2.2. Apparatus

The cathodic deposition of SnO_2 film on a copper substrate was performed in a cylindrical electrochemical cell with a capacity of 300 ml as shown in Fig. 1 It was composed of rotating cathode and cylindrical graphite act as an anode located in a cell body with dimensions (length=12cm, diameter=8cm). The cathode was a copper cylinder substrate with an outside diameter of 1.8cm, a length of 1 cm, and a thickness of 0.5 mm fixed on a stainless-steel rod has an outside diameter of 1.7cm and length of 9cm attached to an electric motor (PHOEN RSO 20D, Korea) with variable speed type. DC power supply type (UNI-T: UTP3315TF-L) was used for supplying the current. A voltmeter type (UNI-UT90A, Hong Kong) was used to measure the exact value of current across the cell. The same system was used in the anodizing stage with making the tin-plated copper act as anode and graphite cylinder act as cathode.

2.3. Electrode preparation

The tin electrodeposition was carried out following the methodology described in the literature [14]. 150 ml of aqueous solution was used as an electrolyte for deposition of SnO_2 film. It was composed of 67.5 g/L tin chloride, 57.5 g/L trisodium citrate and 0.05 g/L Thiourea. Thiourea was introduced into the precipitation bath as a grain refiner to improve the quality of the deposited layer. Firstly, copper surface was polished with sandpapers of 400 and 800 grits then cleaned by immersion in an ultrasonic bath containing ethanol and acetone for 15 min to remove organic contaminants. After that it was activated in 1M HCl for 5 min followed by rinsing thoroughly with deionized water and dried. The cathodic deposition started by applying a current density of 3 mA/cm^2 on the cathode using DC power supply for a period of 50 min at a temperature of 40 ºC. At the end of deposition, copper cylinder coated with tin film was dismantled from the stainless-steel rode, washed several times by distilled water then dried at 70 ºC for 1 h. The copper cylinder coated with tin was then anodized using 200 ml oxalic acid solution at different concentration, various voltage, time of anodizing, and rotation.

2.4. Characterization

The morphology and structural properties of the fabricated porous tin oxide nanofilms were examined using field emission scanning electron microscopy (FE-SEM) equipped with energy-dispersive X-ray spectroscopy (EDS) for elemental analysis. The crystalline phases of the fabricated layers were determined using X-ray diffraction (XRD) with Cu Kα radiation. The surface roughness was identified by atomic force microscopy (AFM).

2.5. Electrochemical decolorization test

The activity of prepared Cu/SnO_2 anodes was evaluated by anodic oxidation of an aqueous solution containing methylene blue at a concentration of 50 mg/L with addition of 35.5g/L sodium sulfate as a supporting electrolyte. The system used in this stage is the same system used in section 2.2 with making the Cu/SnO_2 cylinder acts as an anode and hollow stainless-steel cylinder (inside diameter of 3.8 cm and length of 5cm) acts as a cathode. The anodic oxidation was conducted at a current density of 20 mA/cm^2 for 120 min. During the oxidation 1 ml of solution was taken every 20 min then diluted 10 times. The concentration of methylene blue was measured via determining the absorbance of the sample at a wavelength of 665 nm using UV-spectrophotometer type (Shimadzu/Japan UV-Vis spectrophotometer) then the concentration can be found from a calibration curve shown in Fig. 2.
The methylene blue removal efficiency was evaluated using Eq. 1.

$$RE\% = \frac{C_o - C_f}{C_o} \times 100 \quad (1)$$

Where C_o represents initial Methylene blue concentration (50mg/L) while C_f represent the concentration of methylene blue in mg/L at the end of experiment.

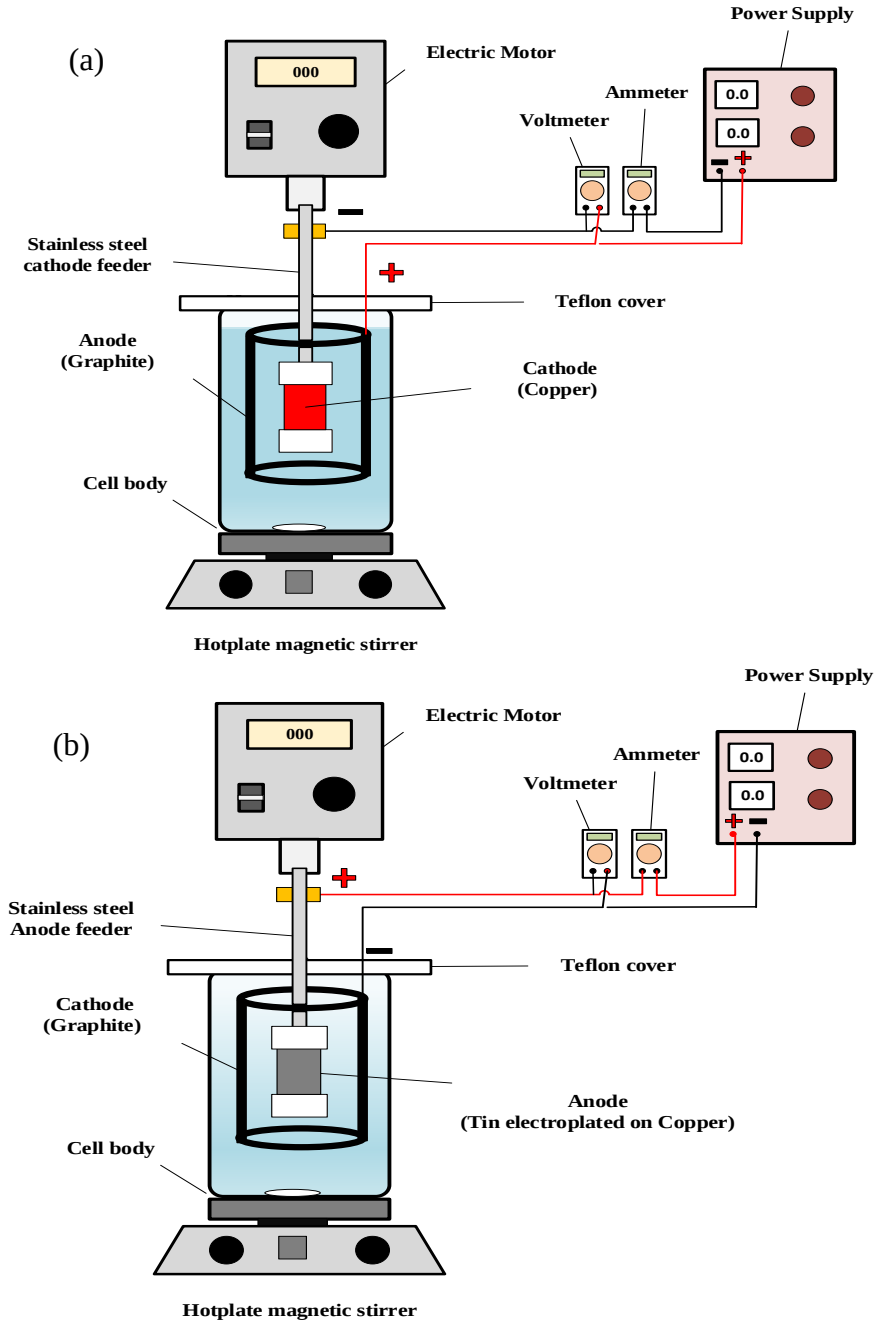

Fig. 1. Electrochemical system for making tin oxide anode a) tin plating system, b) tin anodizing system

3- Results and discussion

3.1. Effect of OA concentration on the electrochemical activity of SnO_2

The concentration of oxalic acid (OA) plays a crucial role in controlling the kinetics of anodic film growth, pore formation behavior, and the resulting electrochemical performance of SnO_2 films. Fig. 3 shows the decay of current at different OA concentrations during the anodizing process where current peaks were observed for all curves. Additionally, increasing of OA concentration resulted in increase the peak of current as well as the final value of current (steady state). The values of average current at steady state were plotted against the concentration of AO as shown in Fig. 4. A linear dependence between average current and OA concentration was observed with R^2 equal to 0.992 confirming that the reaction kinetics is limited by mass transfer in the electrolyte [11]. This linear dependence

could be explained by the fact that average current value is a reveal of inner status of charge transfer which related with forming and dissolving tin oxide as well as oxygen evolution at the tin anode [19].

Fig. 5 shows that the final MB concentration during degrading of MB using SnO_2 anode is decreased with increasing of OA concentration used during the anodizing. Table 1 shows the decolorizing efficiency of MB using SnO_2 anodes prepared at different OA concentrations where higher efficiency can be obtained when using anodes prepared at higher concentration of OA. However, using OA at a concentration of 0.5 M has a little effect on the MB degradation confirming the SnO_2 anode prepared by anodizing share the same properties when the concentration of OA is between 0.4 M and 0.5 M. From an economical perspective, using 0.4 M would be more suitable for further investigation the effect of other anodizing parameters.

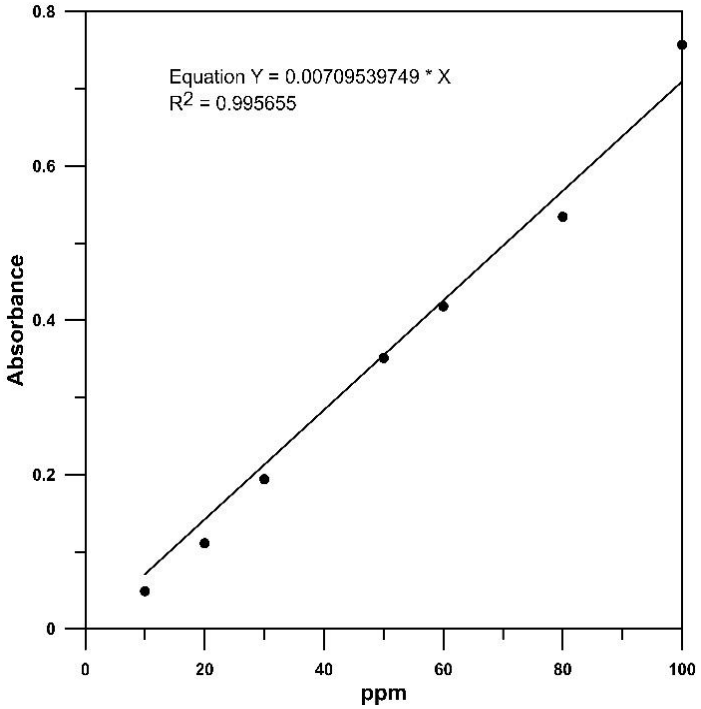

Fig. 2. Calibration curve

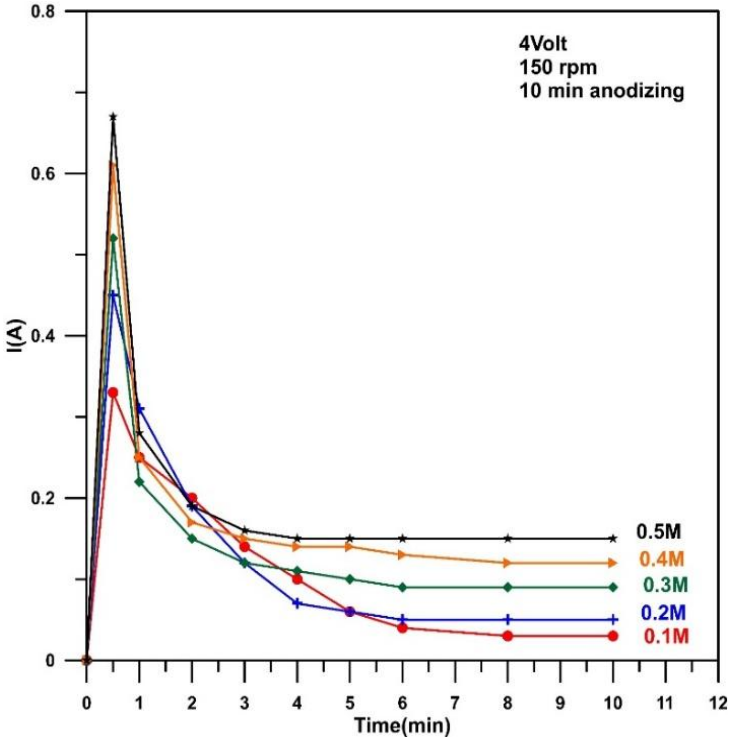

Fig. 3. Current decay with time at different OA concentrations

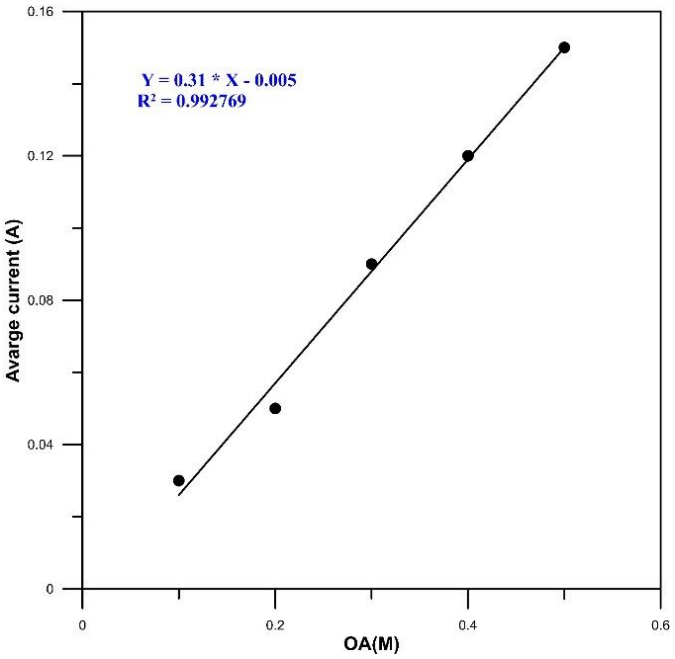

Fig. 4. Average current vs. OA concentration

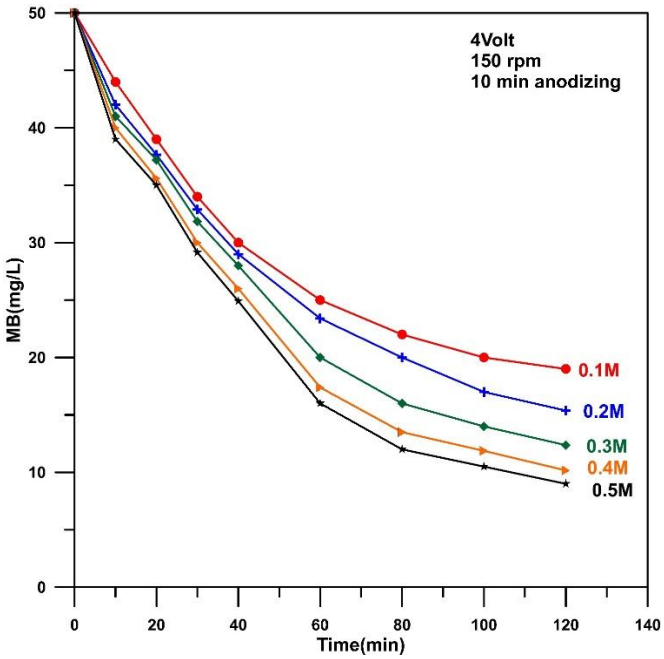

Fig. 5. Effect of OA concentration on SnO_2 activity

Previous studies confirmed that using OA concentration up to 0.4 M gives a regular, crack-free structure where OA acts as a chelating agent, forming soluble tin-oxalate complexes that promote the localized dissolution [20]. Furthermore, previous studies confirmed that increasing the concentration to 0.5 M resulted in structural deterioration and surface cracking, attributed to excessive chemical dissolution causing pore wall collapse [14]. Additionally, high concentrations (>0.4 M) intensify the oxygen evolution reaction (OER), generating gas bubbles that cause internal stress and crosswise cracks, as demonstrated by Cao et al. [12].On the other hand, Zaraska, et a. [11] found that more concentrated acid results in more open porous structure with average diameter of Nano-pores remains approximately constant as concentration of acid exceeds 0.3 M.

3.2. Effect of applied voltage on SnO_2 electrochemical activity

The applied potential serves as the principal driving force in the anodizing process, as it dictates the magnitude of the effective electric field across the barrier layer. Furthermore, it directly regulates the interplay between the ionic current, which governs oxide growth, and the electronic current, which is responsible for gas-evolution

reactions. This physicochemical balance ultimately shapes the resulting pore architecture and determines the electrochemical efficiency of the anode in degrading organic contaminants such as methylene blue (MB). Fig. 6 shows the decay of current at different applied voltages during the anodizing process where increasing the applied voltage resulted in increase the peak of current as well as the final value of the anodizing current

Table 1. decolorizing efficiency of MB using SnO_2anode prepared at different OA concentrations

OA concentration	MB decolorizing efficiency (%)	Final MB concentration (mg/L)
0.1	62	19
0.2	69.24	15.38
0.3	75.2	12.37
0.4	79.66	10.17
0.5	82	9

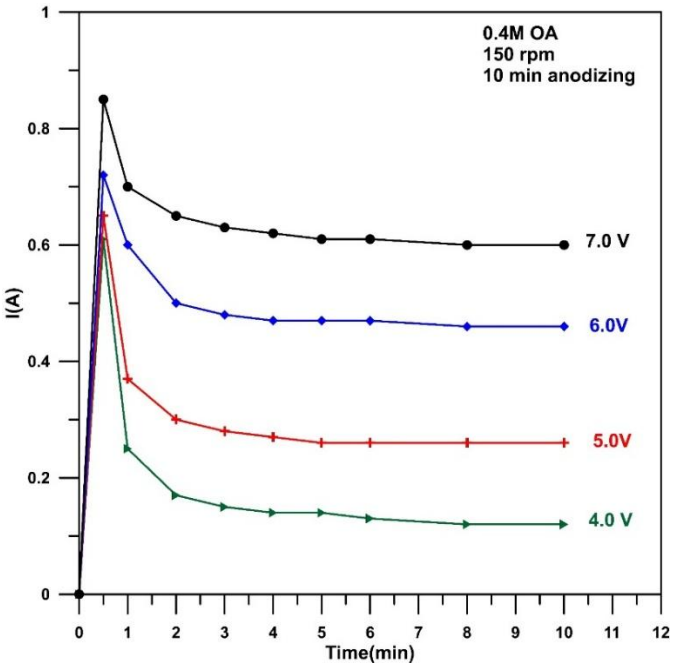

Fig. 6. Current decay with time at different voltages

The I–t transients Fig. 6 clearly demonstrate the kinetic sensitivity of the anodizing system to variations in the applied potential. When the voltage is increased from 4 to 5 V, the current exhibits an immediate and pronounced rise, reflecting the rapid enhancement of the electric field across the barrier layer and the accelerated initiation of oxide nucleation. At moderate potentials (4–5 V), this initial surge is followed by a smooth decay toward a steady state, indicating that ion-migration–controlled oxide growth dominates and promotes the formation of uniform and compact porous layer [19, 21]. In contrast, higher voltages (6–7 V) introduce noticeable fluctuations in the current profile, signifying a shift toward increased electronic conduction and intensified oxygen-evolution activity within the confined pore channels [21]. As reported by Cao et al., [23], such current instabilities are directly associated with the development of segmented pore structures and internal voids, arising from the mechanical stress exerted by gas accumulation within the growing oxide matrix. Zarei, et al. [24] found that applying voltage of 8 V results in poor adhesion of oxide on the substrate using OA electrolyte due to more vigorous O_2 evolution also number of cracks increased as the voltage exceeded 8V.

The values of average current were plotted against the applied voltage, as shown in Fig. 7, where a linear dependence between average current and applied voltage was observed, with R^2 equal to 0.995, confirming that the reaction kinetics is limited by mass transfer in the electrolyte as the voltage increased. Similar trends have been reported in preparing tin oxide by anodizing using different acidic and alkaline media [11, 23, 25-26]. Furthermore, the relation between maximum peak of current and applied potential seems to be an exponential as shown in Fig. 8 Same behavior was noted by Zaraska, et al. [27].

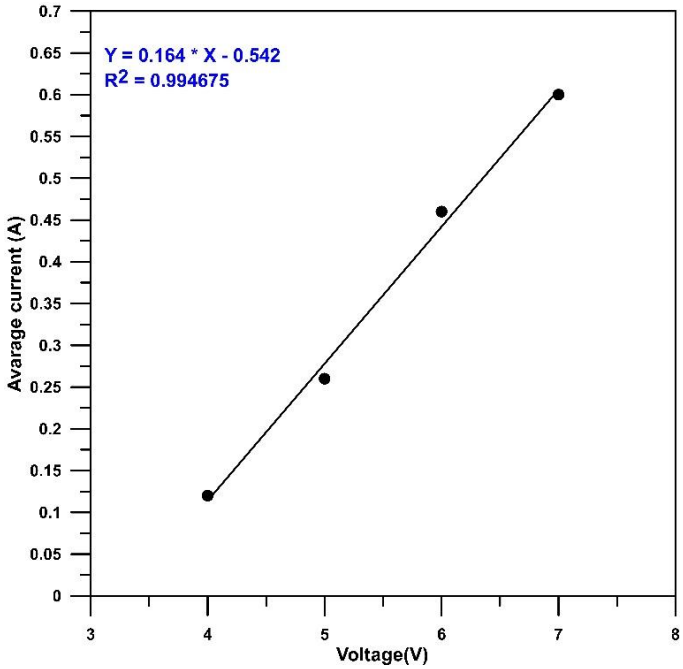

Fig. 7. Average current vs. applied voltage

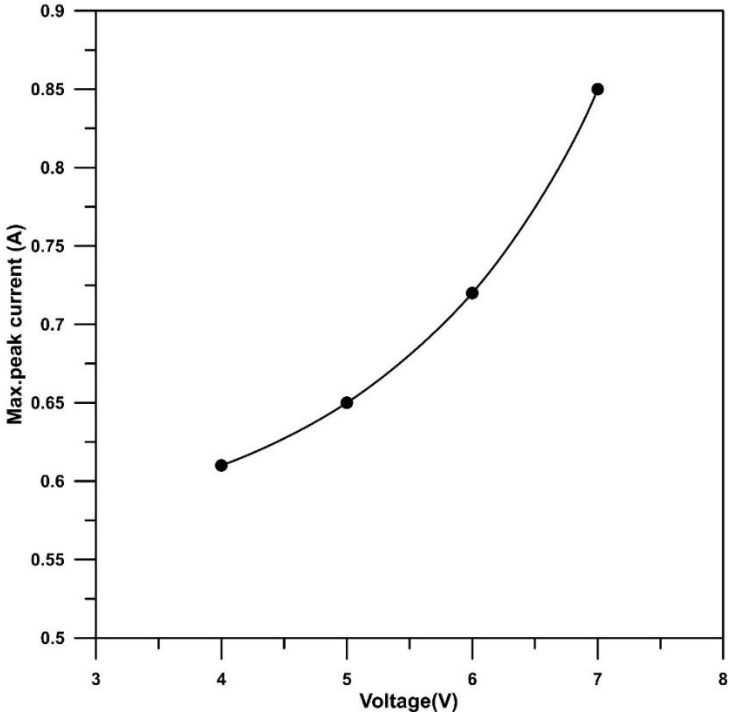

Fig. 8. Maximum peak current vs. applied voltage

The degradation profiles Fig. 9 clearly demonstrate the superior performance of the sample anodized at 5 V, which exhibits the highest removal efficiency of methylene blue (MB) within the first 10 minutes. This enhanced activity is attributed to a regulated local dissolution mechanism, wherein the applied potential of 5 V establishes an optimal balance between metal oxidation at the metal/oxide interface and field-assisted chemical dissolution at the pore base. Such a balance is essential for sustaining uniform pore propagation and preventing structural instabilities. As reported by Zaraska et al. [30] maintaining this equilibrium is critical for generating open, well-defined nanochannels with consistent diameters, thereby facilitating unobstructed diffusion of MB molecules toward the deeper active sites within the porous SnO_2 framework. Although high voltages ($\geq$ 7 V) lead to an increase in oxidation current, this increase does not necessarily translate into enhanced oxidizing activity. Rather, it may lead to pore wall collapse and thinning due to accelerated lateral dissolution, as described by Shen et al., [14]. Previous studies showed that, at voltage higher than 6 V, structural defects and transverse cracks resulting

from oxygen release begin to impede charge transport pathways and undermine the stability of the pore structure [9, 27].

Table 2 displays the decolorizing efficiency of MB using SnO_2 anodes prepared at different applied voltages where higher efficiency can be obtained when using anodes prepared at higher applied voltage. However, applying voltage higher than 5 V has a little effect on MB degradation so from an economical perspective, applying voltage of 5 V would be more suitable for further investigating the effect of other anodizing parameters.

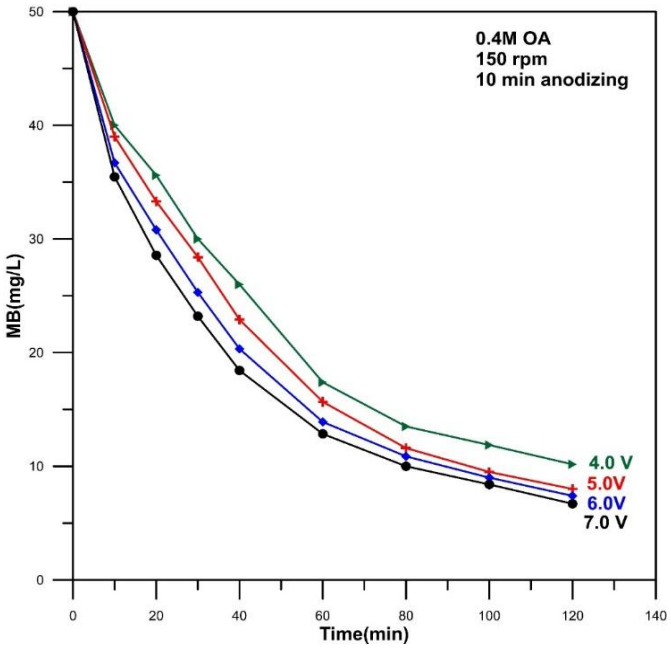

Fig. 9. Effect of applied voltage on SnO_2 activity in removal of MB

Table 2. Decolorizing efficiency of MB using SnO_2 anode prepared at different applied voltage

Applied voltage (Volt)	MB decolorizing efficiency (%)	Final MB concentration (mg/L)
4	79.66	10.17
5	84	8
6	85.2	7.4
7	86.6	6.7

3.3. Effect of time on SnO_2 electrochemical activity

The anodization duration is a decisive parameter that controls the total charge passed through the cell, governing not only the film thickness but also the intricate architectural evolution of the pore walls and diameters. In this study, anodization was performed at 5.0 V for 10, 15, and 20 minutes. The current-time transients Fig. 10 display a reproducible decay followed by a steady-state regime for all durations.

This behavior signifies the establishment of a dynamic equilibrium between the oxidation of metallic tin at the substrate interface and the field-assisted dissolution of the oxide at the pore solution interface [27]. Previous works reported that increasing anodization time resulted in increasing thickness and pore development of SnO_2 films [26]. Chen, et al., [28] investigated the effect of time (1, 3, 5, and 7min) on the morphology of tin oxide and found that at 1 min cracks and incompact nano pores structure was observed but with prolongation a more regular and uniform structure was formed because the rates of anodization and dissolution are reached a dynamic balance. Fig. 11 shows the decay of MB concentration with time when using SnO_2 anodes prepared at different anodizing times. All curves exhibited similar behavior with increasing MB removal as time of anodizing increased.

Table 3 displays the decolorizing efficiency of MB using SnO_2 anodes prepared at different anodizing times where higher efficiency can be obtained when using anodes prepared at longer time. However, using anodizing time higher than 15 min has a little effect on MB degradation consequently from an economical perspective, anodizing for 15 min would be more suitable for further investigating the effect of other anodizing parameters.

3.4. Effect of rotation speed on SnO_2 electrochemical activity

Rotation speed in general has an essential effect on the structure of tin oxide formed during anodizing. Rotation of anode can suppress the formation of internal cracks and making rapid liberation of gaseous from Nano-channels. Fig. 12 shows the decay of current with time at different rotation speeds where higher peaks of current were

observed as rotation increased. Moreover, current curves are smoother and well-shaped due to a uniform removal of oxygen from surface of anode as well as an effective electrolyte exchange inside pores. The formation of higher peaks of current with increasing rotation can be interpreted as a much faster transport of ionic species to the metal/electrolyte interfaces [29]. Zaraska, et al., [30] found that tin oxides films formed in a stirred electrolyte showed more uniform morphology with much lower cracks and voids.

The decay of MB concentration with time using SnO_2 prepared at different rotation speeds is shown in Fig. 13 where lower final MB concentration could be obtained using SnO_2 prepared at high rotation speed. The decolorizing efficiency of MB using SnO_2 prepared at different rotation speeds is outlined in Table 4 where increasing rotation gives better removal of MB due to the compact and uniform structures that obtained at high speeds. This can be explained by increasing rotation results in faster transport of ionic species towered the metal electrolyte interface in addition to more uniform removal of O_2 from the surface of anode combined with an effective electrolyte exchange inside the pore of oxide film [30]. Furthermore, increasing rotation can dissipate the joule heat more efficiently which is a significant factor affecting on the growth of oxide [30].

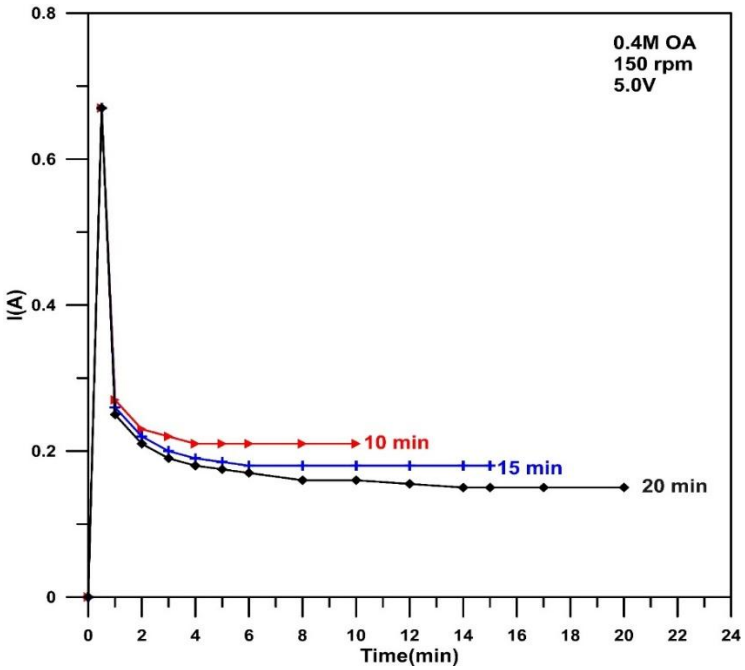

Fig. 10. Current decay with time at different anodizing times

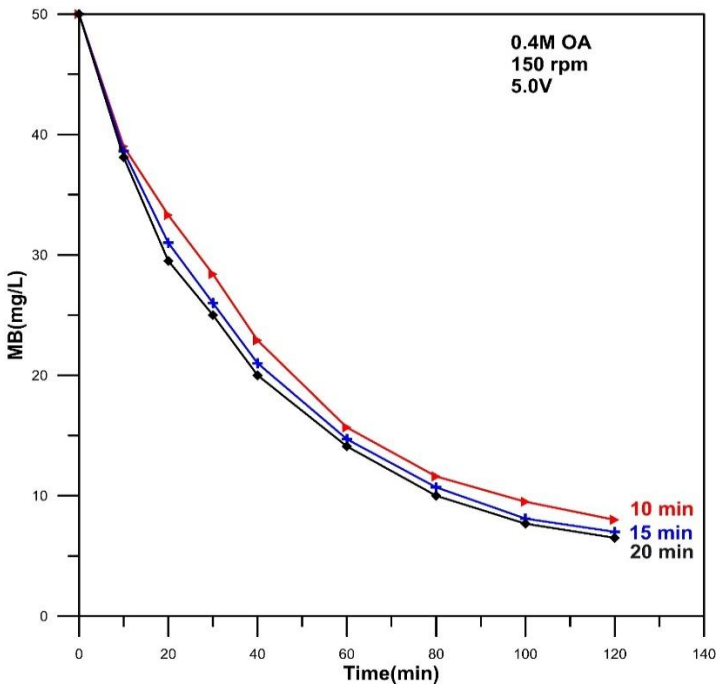

Fig. 11. Effect of anodizing time on SnO_2 activity in removal of MB

Table 3. Decolorizing efficiencies of MB using SnO_2anode prepared at different anodizing time

Time(min)	MB decolorizing efficiency (%)	Final MB concentration (mg/L)
10	84	8
15	86	7
20	86.96	6.5

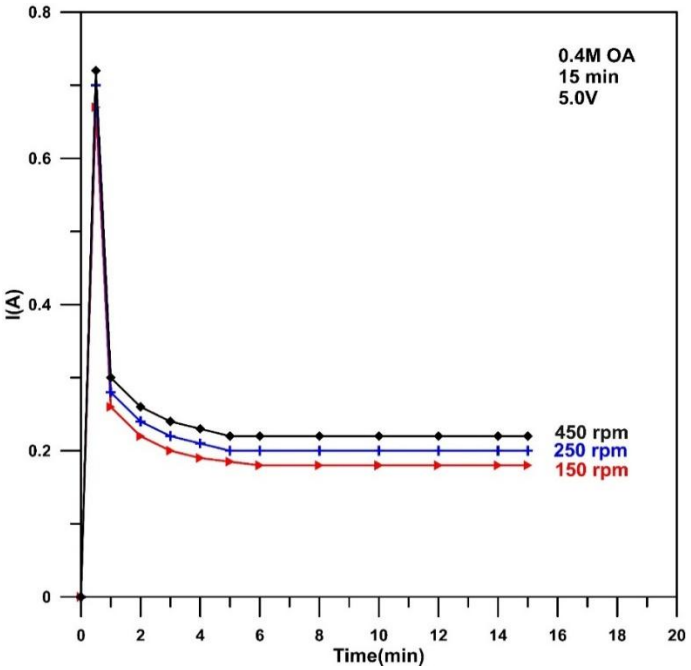

Fig. 12. Current decay with time at different rotation speed

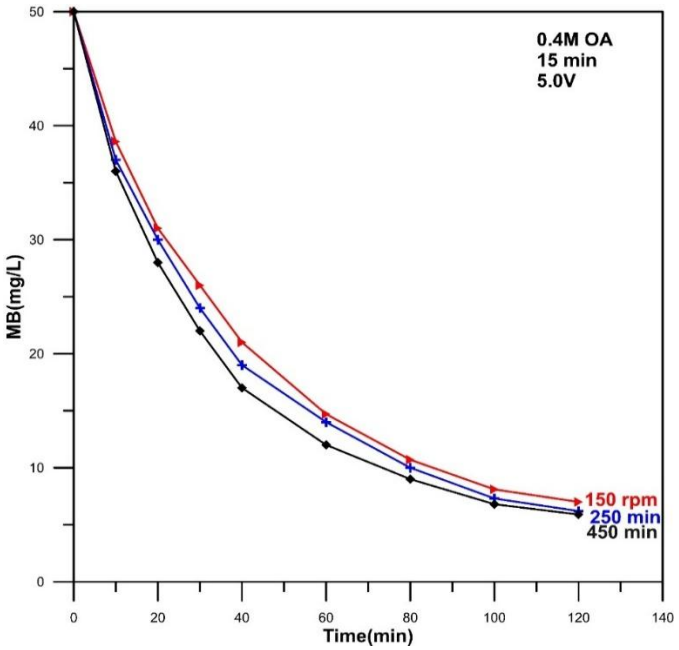

Fig. 13. Effect of rotation speed on SnO_2 activity in removal of MB

3.5. Characterization of SnO_2

Fig. 14 displays the XRD results for Cu/SnO_2 anodes prepared by anodizing at potential of 5 V, 0.4M OA, 15 min, and 250 rpm. Several weak peaks were observed at 2θ= 26.55º (110), 37.65º (200), 57.15º (002), 64.55º (112), and 66.15º (301) which can be tentatively assigned to tetragonal rutile SnO_2 (PDF no. 41-1445) [1, 26]. Two strong β-Sn peaks were observed at 2θ= 30.55º (200) and 31.95º(101), in addition to weaker peaks at 2θ= 44.85º(211), 62.45º(112),and 63.75º(400), consistent with (PDF no. 04-0673)[28]. Peaks for copper were also observed at 2θ= 43.15º (111), 50.25º(200), and 73.95º(220), consistent with (PDF no. 04-0836) [1].

Similar results have been observed in previous studies [1, 25, 27]. A crystalline phase of β-Sn was also observed, consistent with some previous studies that prepared SnO using other electrolytes [26]. The results showed that the resulting SnO_2 layer had weak peaks, indicating an amorphous (weak crystallinity) structure [23, 27, 28]. Zaraska et al. [27] obtained similar results when SnO_2 was prepared by anodization using oxalic acid. Cao et al. [12] also found that the SnO_2 layer had a low-order, amorphous, or weakly crystalline structure when prepared from a solution containing fluoride (F^-) and sulfide (S^{2-}) ions.

Table 4. Decolorizing efficiencies of MB using SnO_2anode prepared at different rotation speed

rotation speed (rpm)	MB decolorizing efficiency (%)	Final MB concentration (mg/L)
150	86	7
250	87.6	6.2
450	88.2	5.9

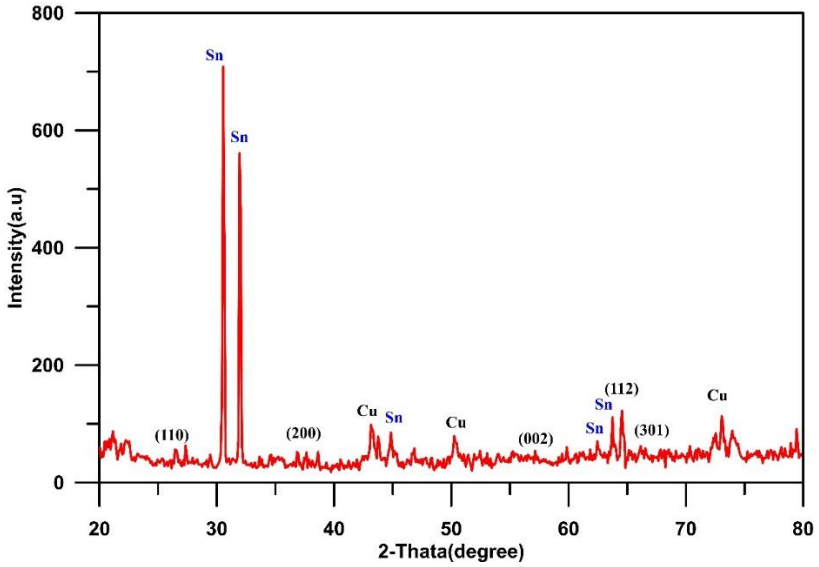

Fig. 14. XRD of Cu/SnO_2 anode

Fig. 15 shows the SEM, EDS, and AFM results for SnO_2 anode prepared at potential of 5 V, 0.4M OA, 15 min, and 250 rpm. Fig. 15 a shows that the oxide layer has a coarse, heterogeneous structure composed of irregularly shaped particles ranging in size from microscopic to nanoscale. This structure indicates that oxidation in an oxalic acid medium promotes oxide growth and partial chemical solubility [27]. It was cleared that anodized SnO_2 anode is crack free structure that is different from results obtained from previous studies using NaOH electrolyte due to the effect of rotation which enhance the removal of oxygen leading to uniform porous anodizing structure [30]. Overall, the prepared SnO_2 layer exhibits a porous structure with high surface area, which is advantageous for electrochemical and catalytic applications.

Fig. 15 b shows EDS results in which peaks of Sn and O were observed that belongs to SnO_2. Furthermore, peak of Cu was observed due to the substrate structure. The presence of Al in the EDS spectrum is attributed to contributions from the sample holder and using fixing materials, as well as the relatively high penetration depth of the electron beam during SEM test, rather than its integration into a layer. Fig. 15 c showed the AFM analysis for the prepared anode where a homogenous nanostructured with high roughness and porosity was observed in which root mean square (RMS) roughness of 28.4 nm was recorded. These results indicate that improve active surface area with good catalytic properties was achieved by adopting the present method for making SnO_2 anode. The average RMS of SnO_2 film measured by AFM was identified to be in the range of 13.7 -34 .2 nm according to the preparation method and its conditions [31].

3.6. Comparison with previous works

Table 5 compares previous studies on methylene blue removal using tin oxide (SnO_2) anodes. It is evident that the performance of these anodes is highly dependent on the preparation method, as well as the influence of hydrodynamic conditions. For example, Table 5 shows that the tin oxide anode prepared using the sol-gel method under stationary conditions exhibits lower methylene blue removal efficiency, attributed to its limited surface area and the stagnant condition.

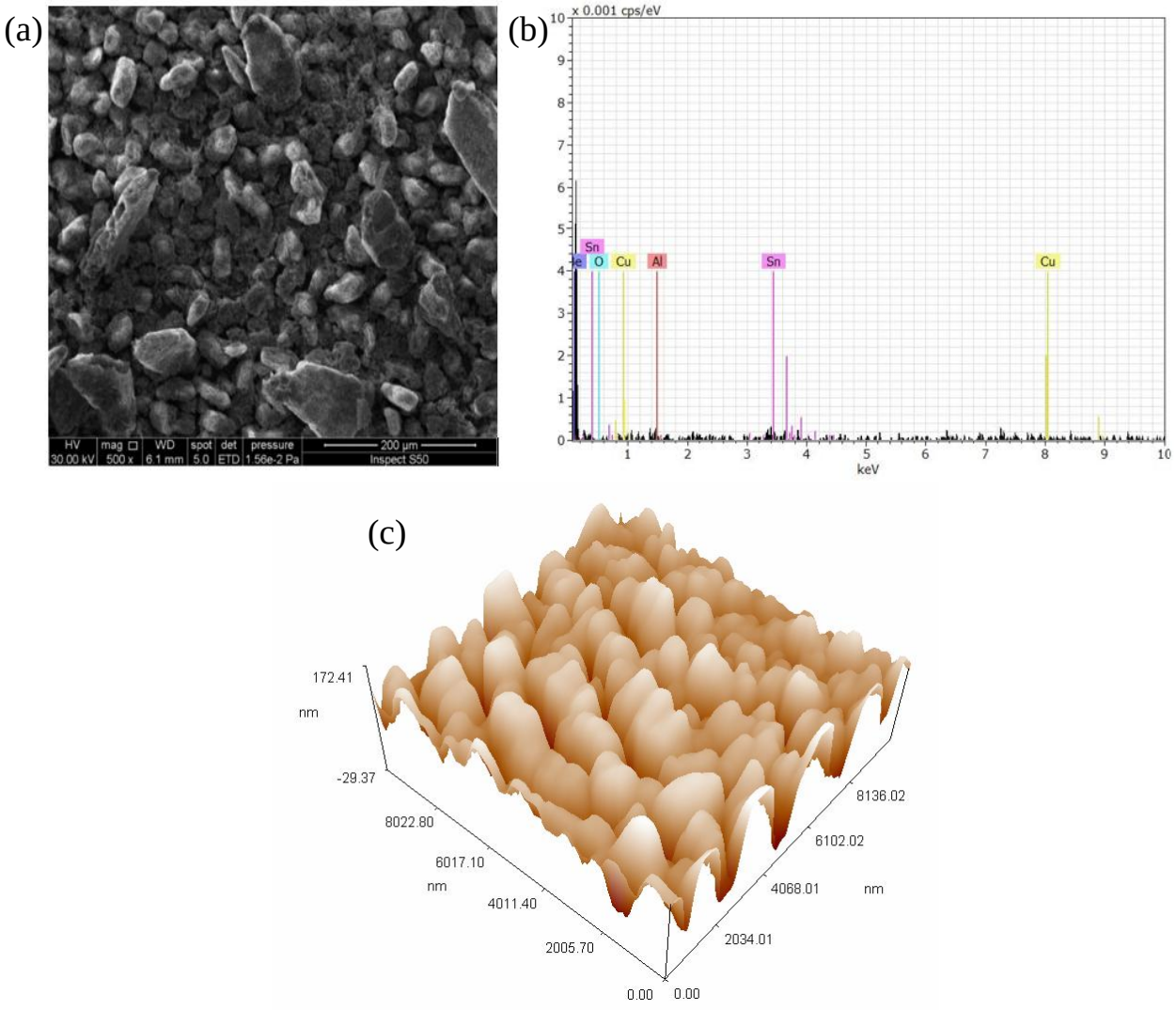

Fig. 15. a. SEM, b. EDS, and c. AFM results for Cu/SnO_2 anode

Table 5. Comparison the performance of SnO_2 anode prepared in this work with previous works

Anode	Method of preparation	Conditions	RE%	Ref.
Ti/SnO_2-Sb stationary	Sol-gel	[MB]o=50 mg/L; Vol. =50 ml, I=20 mA/cm^2; time =100 min	43.8	8
Ti/SnO_2-Sb stationary	Pulse-electrodeposition	[MB]o=50 mg/L; Vol. =50 ml, I=20 mA/cm^2; time =120 min	65.1	32
Pb modified porous. SnO_2 anode stationary	Sol-gel	[MB]o=100 mg/L; ph=5, Vol. =50 ml, I=20 mA/cm^2;time =240 min	94.6	33
Cu/SnO_2 Rotating cylinder anode	DC-electrodeposition+ anodizing	[MB]o=50 mg/L; Vol. =50 ml, I=20 mA/cm^2;250 rpm; time =120 min	87.6	Present work

Furthermore, the application of pulsed electrochemical deposition improved methylene blue removal efficiency due to its uniform structure. Palladium doping yielded better results due to enhanced electrocatalytic activity; however, the use of palladium may raise environmental and toxicity concerns. In contrast, the application of anodizing technique with rotating configuration yielded better results due to the forced convection effect, which reduces the boundary layer thickness during anodizing, and the coarse and porous surface structure of the tin oxide, which increases the number of active sites and thus improves electrolyte access. Overall, this method is characterized by its ability to prepare a tin oxide anode with an excellent structure, capable of organic pollutants degradation at high removal efficiency.

4- Conclusion

A Successful preparation of SnO_2 anode on a copper cylinder was achieved via a one-step anodizing using OA electrolyte combined with rotating cylinder electrode technique. Effects of applied voltage, electrolyte concentration, time, and rotation of anode were investigated. Results showed that the best SnO_2 anode with high electrolytic activity expressed in terms of MB removal can be prepared using anodizing conditions represented by a potential of 5 V, an OA concentration of 0.4M, a time of 15 min, and a rotation speed of 250 rpm in which MB removal of 87.6% was achieved within 120 min.

An increase in the maximum current was observed with increasing each of OA concentration, applied potential, and rotation of electrode. Besides strong linear dependences between average steady state current with OA concentration and applied voltage confirming mass transfer limitation kinetics. Further improving in the activity of SnO_2 anode can be achieved via increasing the rotation speed of anode that facilitates escaping O_2 from the channels of anode film which enhances electrolyte exchange inside the pores of anode. Structure morphology of tin oxide was found to be irregular with crack free structure suitable for electrochemical oxidation processes. The using of rotating cylinder technique seems to be an effective strategy for preparing tin oxide by anodizing method. Furthermore, using metallic film electrodeposited on a cu substrate would be more economic than using titanium substrates.

Acknowledgment

Authors would like to thank the staff of biochemical engineering department at Baghdad university- Iraq, for their helpful and technical support.

References

[1] X. Chen, J. Liang, Z. Zhou, H. Duan, "The preparation of SnO2 film by electrodeposition," *Materials Research Bulletin*, vol. 45, no. 12, pp. 2006-2011, Dec. 2010. https://doi.org/10.1016/j.materresbull.2010.07.029

[2] T. Zhang, L. Liu, Q. Qi, S. Li, "Development of microstructure In/Pd-doped SnO2 sensor for low-level CO detection," *Sensors Actuators B: Chemical*, vol 139, no 2, pp. 287-291, 2009. https://doi.org/10.1016/j.snb.2009.03.036

[3] J.A. Ayllon and M. Lira-Cantu, "Application of MEH-PPV/SnO2 bilayer as hybrid solar cell," *Springer Nature Link*, vol. 95, no. 1, pp. 249–255, Apr. 2009. https://doi.org/10.1007/s00339-008-5023-z

[4] S. T. Chang, I. C. Leo, C. L. Liao, J. H. Yen, and M. H. Hon, "Electrochemical behavior of nanocrystalline tin oxide electrodeposited on a Cu substrate for Li-ion batteries," *Journal of Materials Chemistry*, vol. 14, no. 12, pp. 1821–1826, Jun. 2004. https://doi.org/10.1039/B316459D

[5] M. Batzill and U. Diebold, "The surface and materials science of tin oxide," *Progress in Surface Science*, vol. 79, no. 2–4, pp. 47–154, Jan. 2005. https://doi.org/10.1016/j.progsurf.2005.09.002

[6] X. Chen, G. Chen, and P. L. Yue, "Stable Ti/IrOx−Sb2O5−SnO2 anode for O2 evolution with low Ir content," *The Journal of Physical Chemistry B*, vol. 105, no. 20, pp. 4623–4628, May 2001, https://doi.org/10.1021/jp010038d

[7] H. Xu, Q. Zhang, W. Yan, and W. Chu, "A Composite Sb-doped SnO2 Electrode Based on the TiO2 Nanotubes Prepared by Hydrothermal Synthesis," *International Journal of Electrochemical Science*, vol. 6, no. 12, pp. 6639–6652, Dec. 2011. https://doi.org/10.1016/S1452-3981(23)19708-2

[8] T. Duan, Q. Wen, Y. Chen, Y. Zhou, and Y. Duan, "Enhancing electrocatalytic performance of Sb-doped SnO2 electrode by compositing nitrogen-doped graphene nanosheets," *Journal of hazardous materials*, vol. 280, pp. 304–314, Sep. 2014. https://doi.org/10.1016/j.jhazmat.2014.08.018

[9] L. Zaraska *et al.*, "The effect of anodizing potential and annealing conditions on the morphology, composition and photoelectrochemical activity of porous anodic tin oxide films," *Electrochimica Acta*, vol. 319, pp. 18–30, 2019. https://doi.org/10.1016/j.electacta.2019.06.113

[10] S. Feng, Y. Tang, and T. Xiao, "Anodization, Precursor Route to Flowerlike Patterns Composed of Nanoporous Tin Oxide Nanostrips on Tin Substrate," *The Journal of Physical Chemistry C*, vol. 139, Pages 287-291, 4 June 2009. https://doi.org/10.1021/jp809282w

[11] L. Zaraska, M. Bobruk, M. Jaskuła, and G. D. Sulka, "Growth and complex characterization of nanoporous oxide layers on metallic tin during one-step anodic oxidation in oxalic acid at room temperature," *Applied Surface Science*, vol. 351, pp. 1034–1042, Oct. 2015. https://doi.org/10.1016/J.APSUSC.2015.06.052

[12] J. Cao, C. Wang, Z. Gao, S. Shang, Q. Gu, N. Gao, Y. Wang, H. Ma, "Formation of Nanoporous Anodized Tin Oxide Films in Electrolyte Containing F− and S2−ECS," *Journal of Solid State Science and Technology*, vol. 9, no. 11, p.113013. 2020. https://doi.org/10.1149/2162-8777/abc5f9

[13] A. Yamaguchi, T. Iimura, K. Hotta, "Transparent nanoporous tin-oxide film electrode fabricated by anodization," *Thin* solid *films*, vol.519, no.8, pp. 2415-2420, jun. 2010. https://doi.org/10.1016/j.tsf.2010.11.049

[14] N. Shin, M. Kim, J. Ha, Y. Kim, and J. Choi, "Flexible anodic SnO 2 nanoporous structures uniformly coated with polyaniline as a binder-free anode for lithium ion batteries," *Journal of Electroanalytical Chemistry*, vol. 914, no. March, p. 116296, 2022. https://doi.org/10.1016/j.jelechem.2022.116296

[15] R. Oriol, J. L. Nava, E. Brillas, O. M. Cornejo, and I. Sirés, "Modeling the electrocatalytic nitrate removal in a rotating cylinder electrode reactor," *Separation and Purification Technology*, vol. 340, no. 4, p. 126714, Jul. 2024. https://doi.org/10.1016/j.seppur.2024.126714

[16] A.H. Abbar, R. H. Salman, and A. S. Abbas, "Studies of mass transfer at a spiral-wound woven wire mesh rotating cylinder electrode," *Chemical Engineering and Processing - Process Intensification*, vol. 127, pp. 10–16, May 2018. https://doi.org/10.1016/j.cep.2018.03.013

[17] J. P. Fornés and J. M. Bisang, "Electrochemical production of colloidal sulphur by oxidation of sulphide ion at lead coated-2- and -3-dimensional rotating cylinder anode surfaces," *Chemical Engineering and Processing-Process Intensification*, vol. 243, pp. 90–97, Jul. 2017. https://doi.org/10.1016/j.electacta.2017.05.050

[18] F. H. Abd and A. H. Abbar, "An innovative combination of anodic oxidation using Cu/SnO2–Sb2O5 rotating cylinder anode with TiO2 photocatalytic process for treating hospital wastewater," *Journal of Industrial and Engineering Chemistry*, vol. 145, pp. 668–685, May 2025. https://doi.org/10.1016/J.JIEC.2024.10.064

[19] C. Lu, J. Wang, D. Meng, A. Wang, Y. Wang, and Z. Zhu, "Tunable synthesis of nanoporous tin oxide structures on metallic tin by one-step electrochemical anodization," *Journal of Alloys and Compounds*, vol. 685, pp. 670–679, 2016. https://doi.org/10.1016/j.jallcom.2016.05.316

[20] L. Zaraska, M. Bobruk, and G. D. Sulka, "Formation of Nanoporous Tin Oxide Layers on Different Substrates during Anodic Oxidation in Oxalic Acid Electrolyte," *Advances in Condensed Matter Physics*, vol. 2015, no. 1, p. 302560, Jan. 2015. https://doi.org/10.1155/2015/302560

[21] P. Li *et al.*, "Growth Model of the Tin Anodizing Process and the Capacitive Performance of Porous Tin Oxides," *The Journal of Physical Chemistry C*, vol. 124, no. 5, pp. 3050–3058, Feb. 2020, https://doi.org/10.1021/acs.jpcc.9b09648

[22] L. Liao, W. Huang, F. Cai, and Q. Zhang, "Preparation and mechanism of honeycomb-like nanoporous SnO2 by anodization," *Journal of Materials Science: Materials in Electronics*, 2021 327, vol. 32, no. 7, pp. 9540–9550, Mar. 2021. https://doi.org/10.1007/s10854-021-05617-y

[23] J. Cao *et al.*, "Morphology evolution of the anodized tin oxide fi lm during early formation stages at relatively high constant potential," *Surface & Coatings Technology*, vol. 388, no. March, p. 125592, 2020, https://doi.org/10.1016/j.surfcoat.2020.125592

[24] M. Zarei, S. Nourouzi, R. Jamaati, I. G. Cano, S. Dosta, and M. Sarret, "Formation of highly uniform tin oxide nanochannels by electrochemical anodization on cold sprayed tin coatings," *Surface and Coatings Technology*, vol. 410, p. 126978, Mar. 2021, https://doi.org/10.1016/j.surfcoat.2021.126978

[25] L Zaraska, K Gawlak, M Gurgul, D Gilek, M Kozieł, RP Socha, GD Sulka, "Morphology of nanoporous anodic fi lms formed on tin during anodic oxidation in less commonly used acidic and alkaline electrolytes," *Surface and Coatings Technology*, vol. 362, pp.191–199, Mar. 2019. https://doi.org/10.1016/j.surfcoat.2019.01.114

[26] M. Wang, Y. Liu, D. Xue, D. Zhang, and H. Yang, "Preparation of nanoporous tin oxide by electrochemical anodization in alkaline electrolytes," *Electrochim. Acta*, vol. 56, no. 24, pp. 8797–8801, Oct. 2011. https://doi.org/10.1016/j.electacta.2011.07.085

[27] L. Zaraska, N. Czopik, M. Bobruk, G. D. Sulka, J. Mech, and M. Jaskuła, "Synthesis of nanoporous tin oxide layers by electrochemical anodization," *Electrochim. Acta*, vol. 104, pp. 549–557, 2013. https://doi.org/10.1016/j.electacta.2012.12.059

[28] H. Chen, W. Zhu, X. Zhou, J. Zhu, L. Fan, and X. Chen, "Formation of porous SnO2 by anodic oxidation and their optical properties," *Chemical Physics Letters*, vol. 515, no. 4–6, pp. 269–273, Oct. 2011. https://doi.org/10.1016/j.cplett.2011.09.035

[29] J. Y. Kim *et al.*, "Highly uniform and vertically aligned SnO2 nanochannel arrays for photovoltaic applications," *Nanoscale*, vol. 7, no. 18, pp. 8368–8377, Apr. 2015. https://doi.org/10.1039/c5nr00202h

[30] L. Zaraska *et al.*, "Influence of anodizing conditions on generation of internal cracks in anodic porous tin oxide films grown in NaOH electrolyte," *Applied Surface Science*, vol. 439, pp. 672–680, May 2018. https://doi.org/10.1016/j.apsusc.2017.12.188

[31] K. Juraić, P. Dubček, M. Bohač, A. Gajović, S. Bernstorff, M. Čeh, and D. Gracin, "Surface morphology of textured transparent conductive oxide thin film seen by various probes: visible light, X-rays, electron scattering and contact probe," *Materials*, *15*(14), 4814, 2022. https://doi.org/10.3390/ma15144814

[32] T. Duan, Y. Chen, Q. Wen, and Y. Duan, "Enhanced electrocatalytic activity of nano-TiN composited Ti/Sb–SnO2 electrode fabricated by pulse electrodeposition for methylene blue decolorization," R*sc Advances*, vol. 4, no. 101, pp. 57463–57475, Nov. 2014. https://doi.org/10.1039/c4ra09145k

[33] Z. Hu, C. Guo, P. Wang, R. Guo, X. Liu, and Y. Tian, "Electrochemical degradation of methylene blue by Pb modified porous SnO2 anode," *Chemosphere*, vol. 305, p. 135447, Oct. 2022. https://doi.org/10.1016/j.chemosphere.2022.135447

تحضير قطب انودي من مادة أكسيد القصدير النانوي المسامي بواسطة الأنودة وباستخدام تقنية القطب الأسطواني الدوار

غيداء انس اسماعيل [١،*]، علي حسين عبار [١]

١ جامعة بغداد، كلية هندسة خوارزمي، قسم الكيميائية الاحيائية، العراق

الخلاصة

تم تحضير اقطاب انودية نانوية ومسامية من مادة أكسيد القصدير (SnO_2) كهروكيميائيًا عبر عملية الأنودة للقصدير المعدني المترسب كهربائيًا على ركيزة نحاسية أسطوانية الشكل باستخدام تقنية القطب الدوار الأسطواني. دُرست تأثيرات جهد الأنودة (٤–٧ فولت)، وتركيز حامض الأوكساليك (٠,١–٠,٥ مولار)، والزمن (١٠–٢٠ ثانية)، وسرعة الدوران (١٥٠–٤٥٠ دورة في الدقيقة) على فاعلية الاكسدة الكهروكيميائية لأكسيد القصدير (SnO_2) كقطب موجب في ازالة الميثيلين الأزرق. أظهرت النتائج أن زيادة تركيز حامض الأوكساليك تُحسّن أداء تحلل الميثيلين الأزرق، بينما تُعزز زيادة جهد الأنودة نشاط القطب حتى جهد ٥ فولت، وبعد ذلك لا يُلاحظ أي تحسن في نشاط القطب في تحلل الميثيلين الأزرق. أما زيادة زمن الأنودة فتُحدث تأثيرًا معاكسًا، في حين أن زيادة سرعة الدوران تُعزز النشاط التحفيزي الكهروكيميائي لأكسيد القصدير (SnO_2). كانت أفضل ظروف الأنودة هي جهد ٥ فولت، وتركيز حامض الأوكساليك ٠,٤ مولار، ومدة ١٥ دقيقة، وسرعة دوران ٢٥٠ دورة في الدقيقة، حيث بلغت نسبة إزالة الميثيلين الأزرق ٨٧,٦%. وأكدت البنية المورفولوجية لأكسيد القصدير المُحضر في الظروف المثلى التحويل الكامل للقصدير إلى أكسيد القصدير ذي بنية خالية من الشقوق. تُظهر هذه النتائج أن اعتماد تقنية الأنودة باستخدام الأسطوانة الدوارة لتحضير انودات أكسيد القصدير يُعد استراتيجية واعدة لتصنيع اقطاب انوديه عالية الأداء مناسبة لمعالجة مياه الصرف الصحي.

الكلمات الدالة: غشاء نانوي مسامي، أكسيد القصدير، أنودة، حمض الأكساليك، أزرق الميثيلين، قطب أسطواني دوار.